J Mater Sci (2007) 42:7927–7933
DOI 10.1007/s10853-007-1551-8

Characterization of spray deposited $CoWO_4$ thin films for photovoltaic electrochemical studies

P. K. Pandey · N. S. Bhave · R. B. Kharat

Received: 25 November 2006 / Accepted: 24 January 2007 / Published online: 3 June 2007

Abstract Preparation of Cobalt tungstate ($CoWO_4$) thin film by spray pyrolysis with ammonical solution as a precursor is presented. The phase and surface morphology characterizations have been carried out by XRD and SEM analysis. The study of optical absorption spectrum in the wavelength range 350 – 850 nm shows direct as well as indirect optical transitions in the thin film material. The d. c. electrical conductivity measurements in the temperature range 310–500 K indicate semiconducting behavior of the thin film. The thin films deposited on fluorine doped tin oxide (FTO) coated conducting glass substrates were used as a photoanode in photovoltaic electrochemical (PVEC) cell with configuration: $CoWO_4 \mid Ce^{4+}, Ce^{3+} \mid Pt$; 0.1 M in 0.1 N H_2SO_4. The PVEC characterization reveals the fill factor and power conversion efficiency to be 0.36 and 0.62%, respectively. The flat band potential is found to be –0.18 V (SCE).

Introduction

Metal tungstates MWO_4 (where, M is a 3D divalent transition metal ion with an ionic radius <1 Å) crystallize with the wolframite type of structure which can be described as made up of hexagonal close packed oxygen atoms with certain octahedral sites filled by M^{2+} and W^{6+} cations in an ordered way. Compounds belonging to this family have been studied as gas sensors [1], catalysts [2] or electrochromic systems [3]. Recently, Montemayor and Fuentes [4] reported electrochemical characteristics of lithium insertion into several 3D metal tungstates (M = Mn, Co, Ni and Cu) prepared by aqueous solution. Also, the earlier work in our laboratory [5, 6] showed the use of metal molybdate and tungstate pellets as photoelectrodes in photovoltaic electrochemical (PVEC) cell. Photoelectrochemical (PEC) cells are devices in which solar energy is converted into either electrical or chemical energy through a phenomenon of electrochemical effects. PVEC cell (a type of PEC cell) consists of a semiconductor as photoelectrode, an inert metal electrode and an electrolyte. The electrolyte contains a redox couple, thus after illumination oxidation takes place at the semiconductor photoanode and exactly opposite reaction occurs at the cathode, so that the composition of the reaction remains unchanged. Consequently, there is zero variation in the free energy of the total process. The literature survey further reveals that better solar to electrical conversion efficiency is obtained with photoelectrodes in thin film form [7, 8] because of large surface area and large number of recombination centre in this form of material. In our earlier communications [9, 10] we have reported the PVEC characterization of spray deposited $NiWO_4$ and $NiMoO_4$ thin films. To the author's knowledge, no report has been found so far on the thin film deposition of $CoWO_4$ by spray pyrolysis (SP). Therefore, it has been thought worthwhile to deposit the thin films of $CoWO_4$ by SP process because the process is found to be simple, inexpensive and suitable for mass production [11]. Also, the SP process has been extensively used in the deposition of oxide materials [12]. The aim of this work is to investigate the structural, optical and electrical properties of $CoWO_4$ thin films deposited on glass

---

P. K. Pandey (✉) · N. S. Bhave · R. B. Kharat
Department of Chemistry, RTM Nagpur University,
Nagpur 440033, India
e-mail: pandeykp2003@yahoo.co.uk

Present address:
P. K. Pandey
Department of Chemistry, IIT, Kanpur 208016, India

substrate by SP and finally to use the deposited thin films as photoanode in PVEC cell.

Experimental

Thin film preparation

$CoWO_4$ thin films were deposited on glass substrate obtained from Blue-Star, India by SP process using an apparatus described elsewhere [13]. The precursor solution for $CoWO_4$ thin film was the ammonical solution of the pink colored powdered material synthesized by precipitation method [4]. The substrates used for thin film deposition were ultrasonically cleaned, acetone-treated glass slide. A 25 mL of the precursor solution of (0.05–0.125 M) was sprayed through a specially designed glass nozzle onto the heated glass substrates held at various temperatures ranging from 300–450 °C. Compressed air was used as carrier gas. The flow rate, deposition time, nozzle to substrate distance and frequency of the to-fro motion of the nozzle were kept constant at 5 mL/min, 5 min, 40 cm and 0.29 Hz, respectively. After the deposition, the thin films at ambient temperature were allowed to cool slowly to room temperature and then taken out for further characterizations.

Material characterizations

The as deposited films were first examined under an optical microscope (Leitz Orthoplan Microscope, Switzerland) to confirm the film deposition pattern, its uniformity and adherence to the substrate. The thin films obtained were then sintered in air atmosphere at temperatures 350–450 °C for crystallization, since the as deposited films prepared onto preheated substrates are always amorphous [14]. These sintered thin films were then subjected to X-ray diffraction (XRD) studies (Philips PW-1710 X-Ray diffractometer) using Cu-K_α (radiation source) anode for structural characterization and phase identification. Surface morphology of the films was studied with scanning electron microscope (SEM), model JXA—840A, from JEOL, Japan with acceleration voltage 20 kV. A gold coating was deposited on the samples to avoid charging of the surface. *EDAX measurement of the gold coated thin film was also carried out***.** The film thickness was determined by the weight difference consideration method [12]. Optical absorption and transmission studies were carried out using Hitachi spectrophotometer (UV-Vis., NIR model 330, Japan) in the wavelength range 350–850 nm. To study the electrical properties of the thin films, dark resistivity measurements were taken using the two point probe method in the temperature range 310–500 K. Silver paste was applied to provide ohmic contact with the film.

PVEC cell construction and characterization

For PVEC studies, the $CoWO_4$ thin films deposited on fluorine doped tin oxide (FTO) coated glass slides [15] (sheet resistance 30 Ω/cm^2) were used. The resistivity of the $CoWO_4$ film deposited on FTO glass slides was brought down from $10^7 - 10^2$ Ω.cm by sintering the film under hydrogen atmosphere [16] for 10 h at 400 °C. Using the sintered thin films of $CoWO_4$ as photoanode and platinum plate as counter electrode, following PVEC cell was constructed:

$$CoWO_4 \mid Ce(SO_4)_2, Ce_2(SO_4)_3 \mid Pt \quad 0.1\ M\ in\ 0.1\ N\ H_2SO_4$$

The distance between the photoanode and the counter electrode was 0.5 cm. Water lens was interposed between the lamp and the cell to avoid the heating of the cell. Current–voltage characteristics of the PVEC cell so constructed were measured under the illumination of 150 W tungsten–halogen lamp. All the voltages were measured with respect to standard calomel electrode (SCE). The capacitance–voltage characteristic of the cell was also studied; the PVEC setup has been described elsewhere [17].

Results and discussion

Optimization of deposition parameters

The films deposited below 350 °C at all the concentrations were found to be non-uniform and not adherent to the substrate whereas no film deposition was observed above 350 °C as revealed from the optical microscopic studies taken for the films at a magnification of 200x. Therefore, the substrate temperature for the film deposition was set to be 350 °C. The optical microscopic studies of the deposited films using the precursor solution of various concentrations at 350 °C revealed that the films prepared at concentration above 0.10 M were porous, non-uniform and not adherent to the glass substrate. The film formation was not observed at concentration below 0.025 M. This may be due to unsuitable substrate temperature. At higher concentration, complete thermal decomposition of solution did not take place. Transparent films were obtained corresponding to the concentrations 0.075 and 0.1 M of the precursor solution. It was revealed from the optical microscopic studies that the films obtained from 0.1 M precursor solution concentration were uniform without any agglomeration. Therefore, based on the optical microscopic studies, the thin film deposition temperature was optimized at 350 °C and the precursor solution concentration 0.1 M.

XRD and SEM studies

Figure 1 shows the XRD patterns of the grown film of $CoWO_4$ deposited on the glass substrate at 350 °C and also of the thin film annealed at 450 °C. The spectra in Fig. 1a indicate that the as deposited film is amorphous in nature. After annealing at 450 °C, the film exhibits an XRD pattern, shown in the Fig. 1b, consistent with the polycrystalline triclinic structure of $CoWO_4$. All the peaks in the diffraction pattern are indexed on the basis of JCPDS data card [18]. The observed '*d*' values are in good agreement with the standard '*d*' values. Therefore, the formation and single phase nature of the film are confirmed.

SEM image (Fig. 2a) of the cobalt tungstate thin films clearly indicates that the deposition of material (nucleation) starts around scattered centres and deposits nearly spherical features with crystallite size of approximately 1–2 μm. From these patterns it can be inferred that initially grain type growth starts which continues till the whole surface is almost covered. After this, material is deposited leading to non-uniformity of the film surface. The films deposited are found to be continuous and microcrystalline in nature. Figure 2b is the EDAX pattern of the thin film. The pattern clearly indicates the presence of Co and W as the constituent elements without any impurities in the film. The peak of Au is due to the coating on the surface.

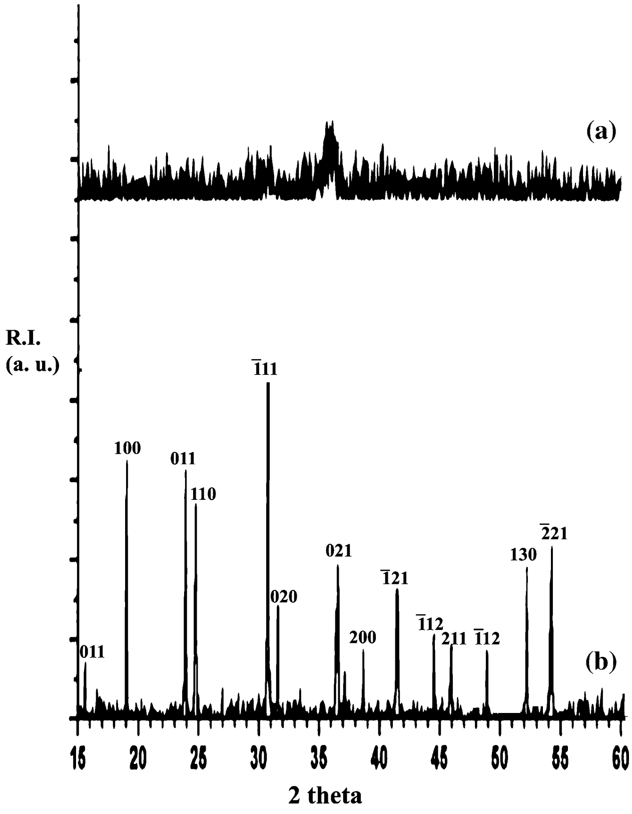

Fig. 1 XRD pattern of $CoWO_4$ thin films (**a**) as deposited (**b**) sintered at 450 °C

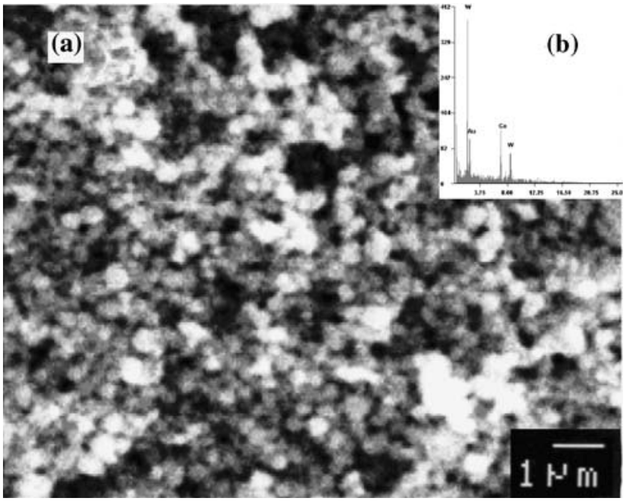

Fig. 2 (**a**) SEM image of $CoWO_4$ thin films (**b**). EDAX patter of the thin film

Thickness of the thin film

The thickness of the prepared thin film was determined using the relation [12] given in Eq. 1,

$$t = m/(A \cdot \rho) \tag{1}$$

where, 'm' is the mass of the thin film deposited onto the substrate, A is the area of the film deposition, '*t*' is the average thickness of the thin film and ρ is the density of $CoWO_4$ which is assume to be the same as that of the bulk material. Thickness of the film is found to be 0.72 μm.

Optical properties

The absorption coefficient, α, for the film is obtained using the relation [19] shown in Eq.

$$\alpha(\lambda) = \frac{10^4}{t}\log_{10}\left[\frac{\{1-R(\lambda)\}^2}{T(\lambda)}\right] \tag{2}$$

where, '*t*' is the thickness of the film, $R(\lambda)$ and $T(\lambda)$ are the reflectance and transmittance at specific wavelength 'λ'. The absorption coefficient is found to be of the order of 10^5 cm^{-1}. To resolve the nature of the optical transmission in the film, the absorption spectrum data are further analyzed as per the theory of Bardeen et al. [20]. The optical band gaps for the deposited $CoWO_4$ thin film are calculated on the basis of the optical spectral absorption using the following well-known relation [21], Eq. 3,

$$\alpha = \mathrm{k}(\mathrm{h}\upsilon)^{-1}(\mathrm{h}\upsilon - \mathrm{E_g})^{n/2} \qquad (3)$$

where, ‘k’ is the constant, ‘E_g’ the energy band gap, ‘hυ’ is the photon energy and ‘*n*’ is equal to 1 for direct bandgap and 4 for indirect bandgap. Figure 3 shows the plot of $(\alpha h\upsilon)^2$ and $(\alpha h\upsilon)^{1/2}$ vs. (hυ) for the $CoWO_4$ thin film. A careful observation of Fig. 3 shows that the fittings might allow to determine the indirect band gap, though few data are aligned along the linear plot for n = 1, but not the direct transition. The plot for n = 4 is linear, indicating an indirect type of optical transition. The values obtained by extrapolating the straight line portion to energy axis at zero absorption coefficients give the indirect optical band gap as 1.45 eV. The direct transition is attributed to spin orbit valence band to conduction band while indirect transition may be due to transition from virtual state in valence band to conduction band minimum [22]. The indirect transition is primarily due to the internal vibration of tungstate ion.

Electrical properties

Ohmic contacts to the $CoWO_4$ thin film are made with silver paste. The electrical resistance was measured in the temperature range 310–500 K. At room temperature the resistivity of the thin film is found to be $10^7 \Omega$.cm. The electrical conductivity (σ) of the film increases with increase in temperature thus indicating semiconducting nature of the thin film material. The plot of log (σ) vs. inverse of absolute temperature, (1/*T*), (Fig. 4) shows a discontinuity in the curve at around 345 K and follows the well known exponential law given in Eq. 4,

$$\sigma = \sigma_o \mathrm{Exp}\,(-\mathrm{E_a}/2\mathrm{k}T) \qquad (4)$$

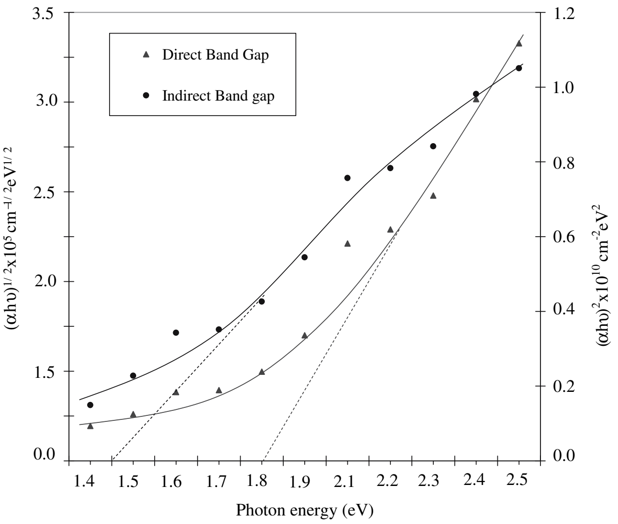

Fig. 3 Plot for optical gap determination of $CoWO_4$ thin film

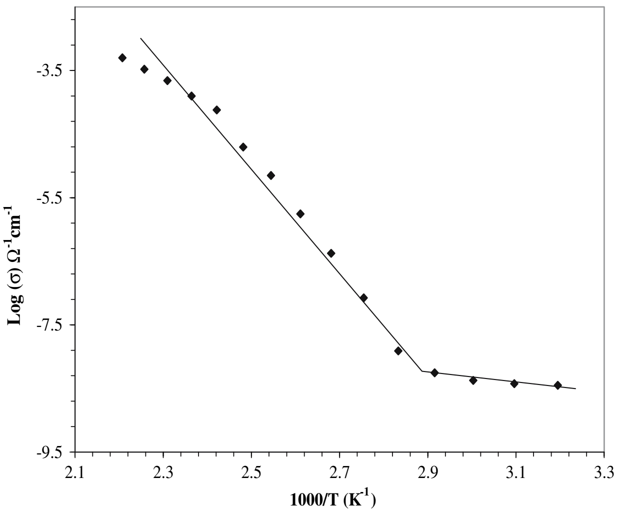

Fig. 4 Plot of Log (σ) vs. 1/*T* for the $CoWO_4$ thin films

The calculated activation energies below and above 345 K are found to be 0.42 eV and 1.56 eV, respectively. The activation energy for conduction is found to be low in the low temperature region. This low temperature conductivity can be considered to be extrinsic (impurity dominated), whereas, conduction in the higher temperature range may be regarded as intrinsic [23, 24]. Therefore, the change in the slope of the plot of log(σ) vs. (1/*T*) is attributed to the change in the conduction mechanism. The two type of competing conduction processes that can be identified in such type of compounds are; (i) conduction by hopping of charge carriers in the narrow 3d band dominating at lower temperature and (ii) normal band like conduction in O^{2-}:2p band which is predominant in high temperature region and is able to suppress the conduction by hopping [25]. Another important cause for extrinsic conduction in the metal tungstate seems to be lattice imperfections and atomic vacancies resulting in slight non-stoichiometry. Atomic vacancies may be cationic or anionic, producing the situation where oxygen or metal ion is in excess, the latter is generally observed for many oxide semiconductors [26].

Selection of suitable electrolyte as redox couple

To constitute the PVEC cell, a suitable redox couple with an appropriate redox potential and optimum concentration is required. It is known that only those redox systems having redox potential values situated within the band gap of the semiconductor can produce a useful semiconductor/electrolyte liquid junction [27]. On the basis of the knowledge of band gap of metal tungstates determined by optical methods and earlier findings with polycrystalline pellets as photoanodes [5, 6], the electrolyte $Ce^{4+}|Ce^{3+}$ was chosen as a redox couple in the PVEC cell configuration. It was observed that the $CoWO_4$ thin film, dipped in 0.1 M $Ce^{4+}|Ce^{3+}$ redox couple at pH = 1 did not show any chemical corrosion or surface damage and maximum photoresponse was obtained at this optimum pH and concentration. Hence, further PVEC studies with $CoWO_4$ thin film photoanode were carried out in 0.1 M $Ce^{4+}|Ce^{3+}$ electrolyte at pH = 1 and H_2SO_4 was used to maintain the pH because electrolytes are sulphate salt of Ce^{4+} and Ce^{3+}.

Effect of illumination intensity on photoresponse of photoanode in PVEC cell

In order to select proper light intensity for illumination of photoanode, the photoresponse of PVEC cell was studied by measuring short-circuit current (I_{SC}) and open circuit voltage (V_{OC}) as a function of light intensity (I_L). The variation of V_{OC} and I_{SC} of PVEC cell with varying light intensity of light source on $CoWO_4$ thin film photoanode is shown in the Fig. 5.

It is evident from the graph that V_{OC} depends upon band bending and change in the photo-fermi level of photoanode, when exposed to light [27]. The intensity dependence of V_{OC} is attributed to changes in surface charge related to oxidation of redox couple on the $CoWO_4$ thin film photoanode resulting in band edge movement. It is further revealed from the graph that above 20 mW/cm^2 light intensity, the photovoltage becomes comparable to the height of the potential barrier for electrons, resulting in the observed saturation of $V_{OC.}$

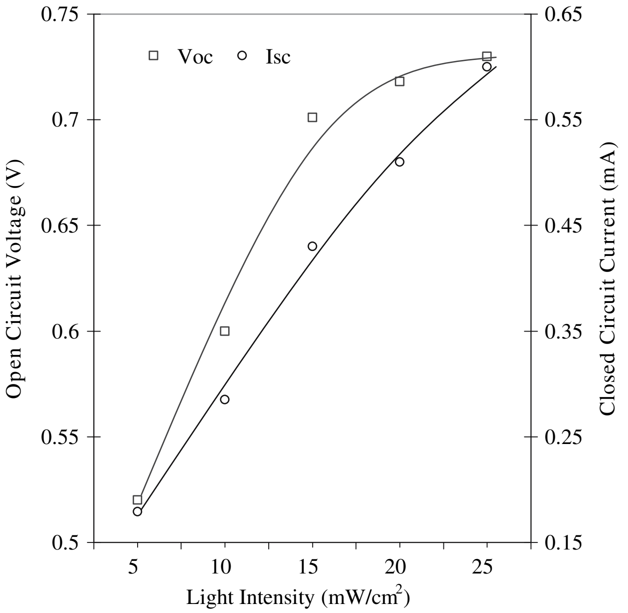

Fig. 5 Variation of I_{SC} and V_{OC} vs. light intensity with $CoWO_4$ thin film as photoanode

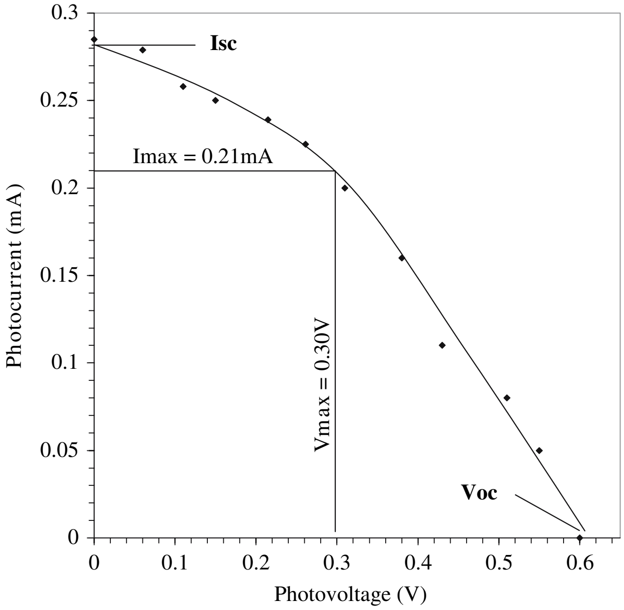

Fig. 6 *I–V* characteristics of PVEC cell with $CoWO_4$ thin films as photoanode

The non linear dependence of I_{SC} on light intensity (beyond 15 mW/Cm^2) indicates that the transport of photogenerated carriers to the semiconductor–electrolyte interface is limiting the rate of overall charge transfer reaction over the range of light intensity employed. According to Kline et al. [28] the observed deviation from linearity of short circuit current with respect to incident light intensity could mainly be attributed to the existence of numerous recombination centres. The flattening of conduction and valence bands as a result of high illumination intensity

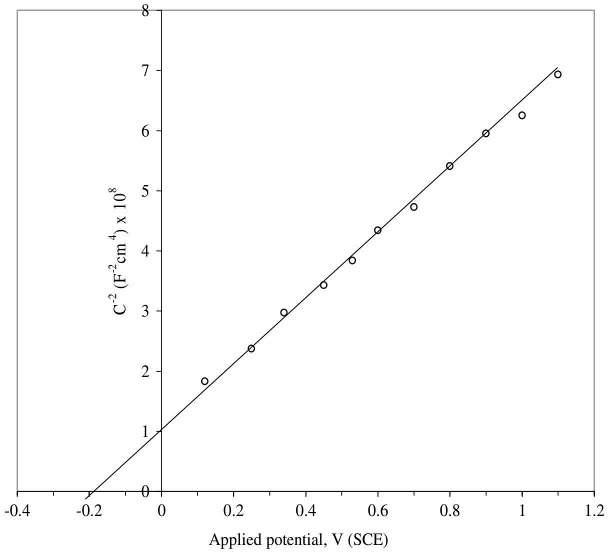

Fig. 7 Mott–Schottky plot

Table 1 Summary of the results obtained for $CoWO_4$ thin films deposited by Spray Pyrolysis process

Characterization results		PVEC cell parameters	
Properties	Results obtained	Parameters	Estimated values
Nature	Polycrystalline	Electrolyte used	$Ce^{4+}\|Ce^{3+}$
Thickness	0.72 μm	Intensity of illumination, I_L	10 mW/cm^2
Absorption coefficient	10^5 cm^{-1}	Short-circuit current, I_{SC}	0.35 mA
Indirect band gap	1.45 eV	Open-circuit voltage, V_{OC}	0.60 V
		Fill factor, *ff*	0.36
Activation energies	0.42 eV (extrinsic)	Conversion efficiency, η%	0.62
	1.56 eV (intrinsic)	Flat band potential, V_{fb}	–0.18 V vs. (SCE)

would reduce the space charge layer field and efficiency of charge carrier separation and thus, reduces the photocurrent. Hence, it was decided to use 10 mW/cm^2 light intensity for photoelectrochemical characterizations of the PVEC cell.

Current–Voltage (*I*–*V*) characteristics of PVEC cell

Current–Voltage (*I*–*V*) output characteristics for the PVEC cell is shown in the Fig. 6. The maximum power output of the cell is given by the largest rectangle that can be drawn inside the curve. The I_{SC} and V_{OC} are found to be 0.35 mA and 0.60 V respectively. The calculations lead to the fill factor (*ff*) of 0.36 and power conversion efficiency (η) of 0.62%. The low efficiency in this investigation might be due to high resistance of the cell, low thickness of the film and interface states, which are responsible for interactive recombination.

Mott–Schottky plot

The semiconductor – electrolyte interface capacitance is measured as a function of applied voltage at frequency of 1 kHz, assuming that the major contribution of the capacitance (*C*) arises from the space charge layer. The data is plotted based on Mott–Schottky relation [29],

$$C^{-2} = 2(\mathrm{q}\epsilon\epsilon_{\mathrm{o}}\mathrm{N_e})^{-1}(V - \mathrm{V_{fb}} - \mathrm{K}T/\mathrm{q}) \quad (5)$$

where, q is the charge, T is the temperature, ϵ is the dielectric constant of the space charge layer, ϵ_o is the permittivity of vacuum, N_e is the charge density, V_{fb} is the flat band potential and V is the applied electrode potential. A linear curve between ($1/C^2$) and applied potential, (Fig. 7), upon extrapolation a give V_{fb} equal to –0.18 V vs. SCE. The V_{fb} determines the maximum cell photovoltage [30] and therefore, it is important for solar cell applications. The low value of V_{fb} in the present investigation is attributed to lower band gap of the material in the thin film form.

Conclusions

The results obtained in the present studies are being summarized in the Table 1. It can be concluded that spray pyrolysis is one of the good methods for the thin film deposition of $CoWO_4$. The films were found to be microcrystalline and single phase after annealing in air at 450 °C, as evident from their XRD spectra and SEM images. The optical study depicts the presence of direct and indirect type of optical transitions in the $CoWO_4$ thin film. The d.c. electrical conductivity measurements reveal the semiconducting nature of the thin film material within the temperature range 310–500 K. The plot of log(σ) vs. ($1/T$) indicates two different type of electrical conduction mechanism in the material. The resistivity of the thin films deposited on FTO coated glass slides can be brought down by sintering the film in hydrogen atmosphere at optimized parameters of temperature and time and then can used as a photoanode in PVEC cell although the power conversion efficiency of the PVEC cell is quite low.

Acknowledgements One of the authors (RBK) is thankful to University Grants Commission (U. G. C.), India for the award of Emeritus Fellowship and the financial support to carry out this research work. We sincerely acknowledge Prof C H Bhosale, Shivaji University, India for providing infrastructural support to carry out few experiments.

References

1. Dusastre V, Williams DE (1999) J Mater Chem 9:965
2. Stern DL, Grasselli RK (1997) J Catal 167:570
3. Kuzmin A, Purans J, Kalendrev R, Paiharey D, Mathey Y (2001) Electrochimica Acta 46:2233
4. Montemayor SM, Fuentes AF (2004) Ceramic International 30:393
5. Pandey PK, Bhave NS, Kharat RB (2005) Matt Lett 59:3149
6. Dhumane WM, Kichambare PD, Kharat RB (1990) J Electrochem Soc Ind 67:612
7. Fress KN (1982) Appl Phys Lett 40:275
8. Liu CH, Wang JH (1980) Appl Phys Lett 36:852
9. Pandey PK, Bhave NS, Kharat RB (2006) Electrochim Acta 51:4659

10. Pandey PK, Bhave NS, Kharat RB (2006) Mater Res Bull 41:1160
11. Subbramaiah S, Raja VS (1994) Sol Energy Mater Sol Cells 32:1
12. Pandey PK, Bhave NS, Kharat RB (2005) Ind J Chem 44A:2034
13. Kiledar VV, Uplane MD, Lokhande CD, Bhosale CH (1995) Ind J Pure Appl Phys 33:773
14. Nunes P, Fernandes B, Fortunato E, Vilarinho P, Martius R (1999) Thin Solid Films 337:176
15. Rajpure KY, Bhosale CH (2000) Mat Chem Phys 64:14
16. Sharon M, Kumar S, Sathe NP (1984) Solar Cells 12:353
17. Pandey PK, Bhave NS, Kharat RB (2006) Ind J Pure Appl Phys 44:52
18. JCPDS-ICDD File No. 72-0479 (2001)
19. Mahmaud SA, Akl AA, Kamal H, Abdel-Hady K (2002) Physica B 311:366
20. Bardeen J, Blatt FJ, Hall LH (1956) In: Breeckenridge R, Russel B, Halm T (eds) Photoconductivity conf. Wiley, New York
21. Moss TS (1961) Optical properties of semiconductors, chap. 3. Butterworth, London
22. Arora SK, Mathew T, Batra NM (1989) J Phys Chem Solids 50:665
23. Bharati R, Singh RA (1982) J Mater Sci 16:511
24. Yadao RB (1983) J Phys Chem Solids 44:697
25. Bharati R, Shaker R, Singh RA (1980) Pramana 14:449
26. Pandey PK, Bhave NS, Kharat RB (2005) Ind J Chem 44A:1186
27. Gerischer H (1983) J Electroanal Chem Soc 150:553
28. Kline G, Kam KK, Ziegler R, Parkinson BA (1982) Sol Energy Mat 6:337
29. Wilson JR, Park SM (1981) J Electrochem Soc 128:2369
30. Arora SK, Mathew T, Batra NM (1990) J Phys D Appl Phys 23:460